Chin. J. Astron. Astrophys. Vol. 5 (2005), No. 2, 159–164
(*http://www.chjaa.org*)

Chinese Journal of
Astronomy and
Astrophysics

First MERLIN Observations of Line Emission from the OH Megamaser toward IRAS 10173+0828

Zhi-Yao Yu

Shanghai Astronomical Observatory, Chinese Academy of Sciences, Shanghai 200030
zyyu@center.shao.ac.cn
National Astronomical Observatories, Chinese Academy of Sciences, Beijing 100012

Received 2004 August 11; accepted 2004 November 5

Abstract Many galaxies are thought to contain massive black holes, with masses in excess of ten million solar masses, at their centres and warped circumnuclear toruses. The best evidence comes from observing gas or masers rotating rapidly within a circumnuclear torus surrounding a central body. Here we report on the first MERLIN observations of line emission from the OH megamaser toward IRAS 10173+0828. The position of peak flux contours of the OH megamaser is consistent with that of the continuum in IRAS 10173+0828. This means that the OH megamaser is a diffuse unsaturated maser which could amplify the diffuse 18 cm continuum emission with an amplification factor of order unity.

Key words: masers – ISM: molecules – galaxies: nuclei – galaxies: active – galaxies: kinematics and dynamic – galaxies: ISM

1 INTRODUCTION

A new class of extragalactic OH sources was discovered with the detection of broad OH mainline maser emission from IC4553 with an unprecedented isotropic luminosity, $\sim 10^3 L_\odot$ (Baan et al. 1982). Thus IC4553 is almost a million times more luminous than any OH maser source observed so far in the Galaxy, hence the name megamaser. IRAS 10173+0828 is an infrared luminous galaxy. Yu (2003) has examined the infrared characteristics of host IRAS sources of 90 OH megamasers including IRAS 10173+0828. Yao, Seaquist & Kuno (2003) have presented the properties of ^{12}CO(1–0) and ^{12}CO(3–2) line emission from IRAS 10173+0828. They obtained spectra of ^{12}CO(1–0) and ^{12}CO(3–2) for the individual source. Here we report on the first MERLIN observations of line emission from OH megamaser toward IRAS 10173+0828. These emission lines are significant for the study of this type sources, because they are both strong and intrinsically narrow. With high-resolution observations powerful OH megamaser emission has been previously detected in Arp220, IIIZw35, Mrk273, and IRAS 17208–0014, by Lonsdale et al. (1998), Diamond et al. (1999), Yates et al. (2000), and Diamond et al. (1999), respectively.

Previous very-long-baseline interferometry (VLBI) observations and time series analysis of the spectra suggested that the megamasers originate in a rotating circumnuclear torus surrounding a massive object (with over mass M of 1.5×10^7 $M_\odot$ at the center of the Galaxy) (Haschick, Baan & Peng 1994; Watson & Wallin 1994).

The OH megamaser emission from IRAS 10173+0828 is remarkably narrow (FWHP= 39 km s^{-1}) for its strength, and the 1667 and 1665 lines are well separated. The 1667 transition shows two distinct peaks displaced by 100 km s^{-1} one from the other and 463 solar luminosities are radiated in the 1667 MHz line. The ratio of the peak flux for the two lines is 14.6 (Mirabel & Sanders 1987). In Sect. 2 we present the observations. Our results and discussion are given in Sect. 3. Finally our conclusions are stated in Sect. 4.

2 OBSERVATIONS

We observed IRAS 10173+0828 for 2 × 12 hrs on 2002 Jan 24–25 using the seven telescopes of Multi-Element Radio Linked Interferometer Network (MERLIN) of the University of Manchester on behalf of PPARC, including the LOVELL antenna. The point-like quasar 0552+398 was used as the bandpass and flux calibration source. IRAS 10173+0828 was observed by switching between two 4-MHz bands containing 128 frequency channels each. The bands were centred on 1588.5 and 1591.5 MHz. The total time on IRAS 10173+0828 was 14.78 hr. In between each 4 min scan on IRAS 10173+0828, the phase reference source 1015+057 was observed at 1590 MHz using a normal 16 MHz bandwidth, averaged to a single 14.5 MHz channel for data processing, and 0552+398 was observed in all the frequencies and configurations. We processed the data using standard techniques for MERLIN extragalactic line data. MERLIN-specific programs were used for initial calibration and conversion to FITS format. All further processing was done in AIPS (Astronomical Image Processing System). A few bad data have been flagged. One channel in each 4-MHz data set was badly affected by interference, but fortunately this is outside the region containing the signal and is not included in the data presented here. The phase and amplitude of 0552+398 were calibrated and the data were used to derive tables of bandpass corrections for the two 4-MHz data sets. These data also showed that there were no instrumental phase changes associated with observing configuration or frequency changes. We calibrated the amplitude and phase of 1015+057, applied the solutions and bandpass corrections to the IRAS 10173+0828. We then reweighted the data from each antenna in proportion to its sensitivity.

We observe 1015+057 at $10^{\rm h}18^{\rm m}27.8483^{\rm s}$, $+05^\circ30'29.936''$ (J2000) and the pointing position of IRAS 10173+0828 was $10^{\rm h}19^{\rm m}59.9^{\rm s}$, $+08^\circ13'34''$ (J2000). The final absolute position accuracy of the components of IRAS 10173 is 20 mas, plus a signal-to-noise-dependent relative error. We plotted the calibrated visibility amplitudes and phases of IRAS 10173+0828 as a function of the channel number. We also converted the frequency axis to velocity. Using a line rest frequency of 1667.359 MHz, the velocity in channel 64 of the data set observed at 1588.5 MHz is $V_{\rm lsr} = 14179.26$ km s^{-1}. The data centred on 1588.5 MHz line showed a feature at the expected position of the 1667 MHz line but the data centred on 1591.5 MHz had a flat spectrum. These latter data were averaged to a single 3.125 MHz data set, mapped and cleaned to give an image of the continuum emission from IRAS 10173+0828. We also Fourier transformed these continuum data without any cleaning to give a one-channel dirty map, and similarly made a 128-channel dirty map of the data containing the line as well as continuum. We then subtracted the continuum map from each channel of line+continuum data. Finally we cleaned the resulting line-only datacube, using a 200 mas FWHM circular restoring beam to make the maps easier

interpret visually. Note that the natural beam fitted to unweighted data is 286×171 mas. We checked that using a circular beam did not produce any artefacts. Typical noise in a quite channel is $\sigma_{\rm rms}$= 1 mJy beam^{-1}, rising to 2 mJy beam^{-1} in the brightest channel due to dynamic range limitations arising from the sparse coverage of the visibility plane. Neither the maps nor the spectrum showed any line emission at the expected frequency of the 1665 MHz emission. We doubled the sensitivity by averaging every four channels and repeated the subtraction of the continuum and the mapping of the line-only data, but still no new emission was found. So, the data are here presented with the velocities adjusted relative to the 1667 MHz line. We used the AIPS task JMFIT to fit 2-dimensional Gaussian components to each patch of line-only emission that exceeded 3-$\sigma_{\rm rms}$ and found in more than one consecutive channel within one beamwidth in position. For MERLIN spectral data the component position uncertainty is approximately given by the maximum dirty beam width divided by the signal to noise ratio. We estimated the uncertainty by taking three times the errors reported by JMFIT in order to also include errors due to the flux distribution being non-Gaussian. We detect signal at >3-σ in the velocity channels observed. Figure 1 shows the spectrum of the OH megamaser in IRAS 10173+0828 constructed from the interferometric images.

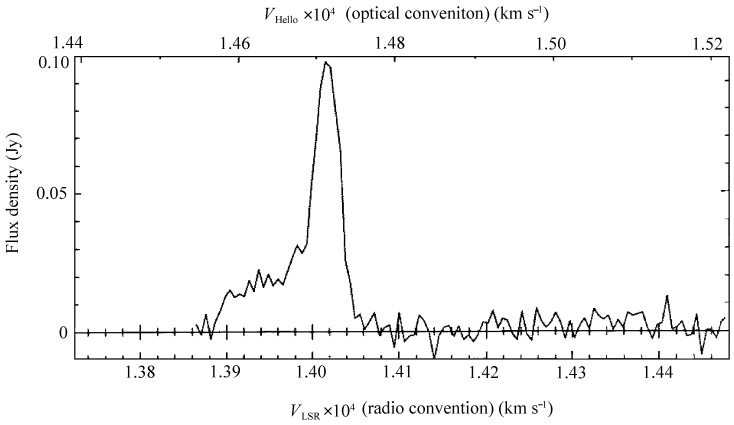

Fig. 1 Spectrum of the OH megamaser in IRAS 10173+0828 constructed from interferometric images.

3 RESULTS AND DISCUSSION

The contour map of OH megamaser toward IRAS 10173+0828 is shown in Fig.2. We subtracted the continuum map for each channel from the line+continuum data. Indicated are the peak flux= 2.0886×10^{-2} Jy beam^{-1} and the contour levels, Levs=2.125×10^{-3}* (–1, 1, 2, 3, 4, 5, 6, 7, 8, 9, 10). Typical noise in a channel is $\sigma_{\rm rms}$ = 1 mJy beam^{-1}, rising to 2 mJy beam^{-1} in the brightest channel due to dynamic range limitations arising from the sparse coverage of the visibility plane. Two clumps have been found at $\sim$ 1.1 arcsec south of the main complex of emission (at about Dec 08°13′32.7″). These are not artefacts but are probably some weak components. Because the two clumps have not been found in the position map of the OH megamaser spots (see following Fig. 3), we will not discuss them further here. From the contour map we find that the contours extend both to the East and the West from the center. The E-W extension of similar amplitude is not related in any obvious way to the beam sidelobe. This

morphology can also be confirmed in the position map of the all OH megamaser spots toward IRAS 10173+0828.

The map (Fig. 3) shows the positions of all the OH megamaser spots toward IRAS 10173+0828 in Fig. 2. In Fig. 3 the size of each circle is proportional to the OH megamaser flux in the corresponding frequency channel. The cross in Fig. 3 marks the position of the continuum emission. Figure 3 shows a map projected on the sky. If a torus is seen edge-on, its projection would just be a line. Figure 3 shows all the OH megamaser spots are separate and distributed in three clumps, the east, central, and west clumps. Within each clump, the OH megamaser spots are almost distributed on a line. Moreover, the three lines run in different directions. Maybe, this means all the OH megamasers in the spots of three clumps are distributed on an edge-on warped circumnuclear torus, for if the torus is not warped the direction of the three different lines in the three clumps would be the same. The direction in Fig. 3 is consistent with the extended direction of the contours in Fig. 2.

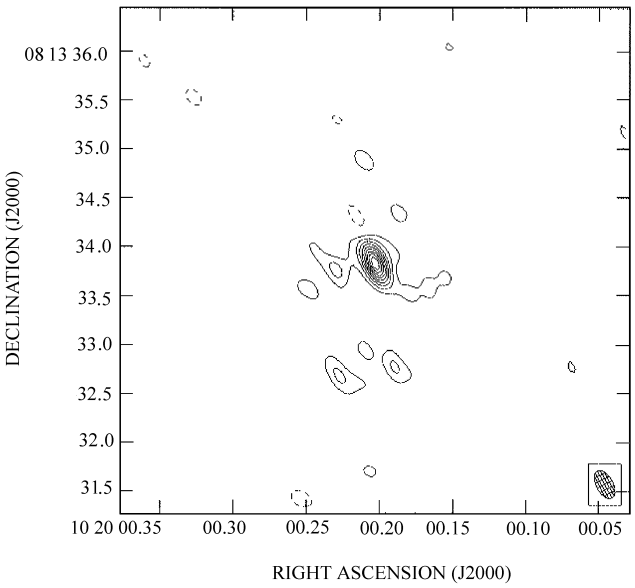

Fig. 2 Contour map of OH megamaser toward IRAS 10173+0828.

We found that neither the maps nor the spectrum showed any line emission at the expected frequency of the 1665 MHz emission. Single-dish observations gave a peak flux ratio of 14.6 for the two lines at 1667 and 1665 MHz (Mirable & Sanders 1987). The LTE value of the ratio is 1.8 (Henkel & Wilson 1990). Thus the OH megamaser toward IRAS 10173+0828 is in non-LTE. The peak flux at 1665 MHz is only (1/14.6) times the one at 1667 MHz. The peak flux at 1665 MHz has been resolved with MERLIN observations, but it is too weak to be detected. The optical depth of the 1665 MHz line may be less than that of the 1667 MHz line. In Table 1 the position errors are 10–20 times larger than that expected from the ratio (beam width)/(signal-to-noise). Only absolute astrometry should be used when comparing the results with other data. The pointing position of IRAS 10173 was $10^{\rm h}19^{\rm m}59.9^{\rm s}$, $+08^\circ13'34''$ (J2000) and 1015+057 was observed at $10^{\rm h}18^{\rm m}27.8483^{\rm s}$, $+05^\circ30'29.936''$ (J2000). The final absolute position accuracy of the components of IRAS 10173 is ∼20 mas, plus a signal-to-noise-dependent relative error.

The continuum contour map of IRAS 10173+0828 is shown in Fig. 4 for comparison with Fig. 2. OH emission consists of two components. One is diffuse unsaturated masers pumped by far-infrared radiation. It is associated with compact continuum emission and is readily explained by the classical OH megamaser model. The other is compact and consists of saturated masers, which is responsible for up to 65 percent of the 1667 MHz flux density. It is not associated with any compact continuum emission, and may be pumped by a combination of collisional and radiative processes (Diamond et al. 1999). The centre of the OH megamaser contour map is at RA(J2000)=$10^{\rm h}20^{\rm m}00.205^{\rm s}$, Dec(J2000)=+08° 13′33.84″, from Fig. 2. The centre of the continuum contour map is at RA(J2000)=$10^{\rm h}20^{\rm m}00.205^{\rm s}$, Dec(J2000)=+08° 13′33.87″, from Fig. 4. The two centres are consistent. Mannucci et al. (2003) showed that the infrared central position was RA(J2000)=$10^{\rm h}20^{\rm m}00.0^{\rm s}$, Dec(J2000)=+08° 13′35.0″, from their table 1. Thus the central positions of both the OH megamaser contour map and the continuum contour map are consistent with the infrared central position. The OH megamaser toward IRAS 10173+0828 is associated with the continuum emission and pumped by the infrared radiation. According to Diamond et al. (1999) the diffuse unsaturated OH megamaser is pumped by the far-infrared radiation and is associated with compact continuum emission. This means that the OH megamaser in IRAS 10173+0828 is a diffuse unsaturated maser which could amplify the diffuse 18 cm continuum emission, with an amplification factor of order unity.

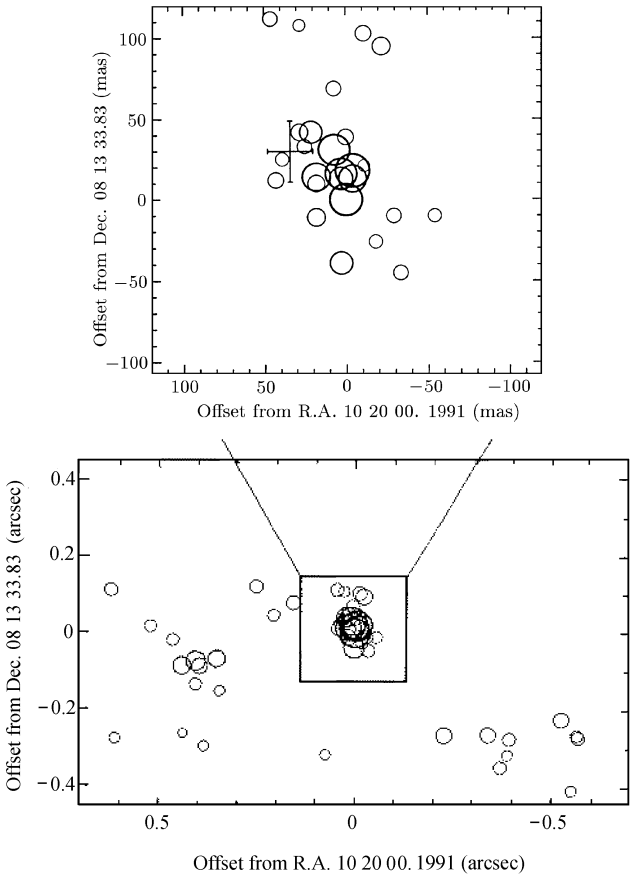

Fig. 3 Map showing all the OH megamaser spots toward IRAS 10173+0828 (the cross marks the position of the continuum emission).

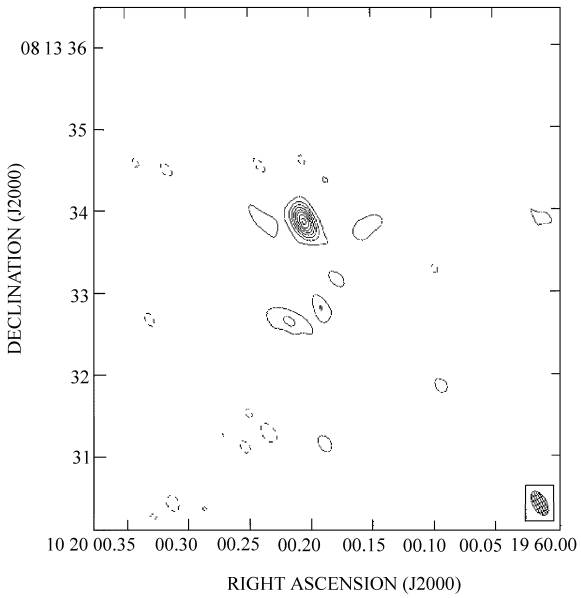

Fig. 4 Contour map of continuum in IRAS 10173+0828.

4 CONCLUSIONS

Here we report on the first MERLIN observations of line emission from OH megamaser toward IRAS 10173+0828. The central position of contour peak flux of OH megamaser is consistent with both the central position of the continuum in IRAS 10173+0828, and the central position of the infrared radiation. The diffuse unsaturated masers are associated with compact continuum emission. This means that the OH megamaser in IRAS 10173+0828 is the diffuse unsaturated maser.

Acknowledgements MERLIN is a national facility operated by the University of Manchester on behalf of PPARC. I thank Dr. Anita M. S. Richards, Dr. P. Thomasson, Dr. T. Muxlow, and all staffs of MERLIN for their kind helps. I also thank the referee for the valuable comments.

References

Baan W. A., Wood P. A. D., Haschick A. D., 1982, ApJ, 260, L49
Diamond P. J., Lonsdale C. J., Lonsdal C. J. et al., 1999, ApJ, 511, 178
Haschick A. D., Baan W. A., Peng E. W., 1994, ApJ, 437, L35
Henkel C., Wilson T. L., 1990, A&A, 229, 431
Lonsdale C. J., Lonsdale C. J., Diamond P. J. et al., 1998, ApJ, 493, L13
Mannucci F., Maiolino R., Cresci G. et al., 2003, A&A, 401, 519
Mirable F. I., Sanders D. B., 1987, ApJ, 322, 688
Watson W. D., Wallin B. K., 1994, ApJ, 432, L35
Yao L., Seaquist E. R., Kuno N., 2003, ApJ, 588, 771
Yates J. A., Richards A. M. S., Wright M. M. et al., 2000, MNRAS, 317, 28
Yu Z. Y., 2003, MNRAS, 338, 745